Int j simul model 21 (2022) 2, 332-340
Original scientific paper

PROCESS PARAMETERS OPTIMISATION FOR SPRING SEAT BASED ON RESPONSE SURFACE METHODOLOGY

Yu, Y. X.; Huang, Y.; Geng, H. H. & Cha, L. L.
Faculty of Mechanical Engineering & Automation, Zhejiang Sci-Tech University, Hangzhou, China
E-Mail: yyxin@zstu.edu.cn

Abstract
Due to the complex structure of spring-seat, six steps were adopted from initial blank to finished product. In this paper, simulation of the stamping process of spring-seat with Dynaform platform was presented and the resulting defects of rupture, wrinkling and spring back were the same as those in a certain factory. Aiming at the wrinkling defects of the helical surface in the forming process, die clearance, blank hold force, and friction coefficient were selected as input variables, wrinkling and thickness uniformity were used as evaluation indexes of stamping quality, and the function relation between the evaluation indices of the stamping quality and variables was obtained through response surface methodology (RSM). After optimisation, the wrinkle index decreased by 31.72 %, and thickness uniformity index decreased by 2.85 %. Stamping validation test was conducted using the optimized stamping parameters. The stamping quality of product was evaluated by gauges. Results showed that spring-seat achieved the quality requirements. The numerical simulation results can provide parameters for manufacturing and reduce the cost in development work.
(Received in January 2022, accepted in April 2022. This paper was with the authors 3 weeks for 1 revision.)

Key Words: Spring Seat, Multistep Stamping Process, Simulation Modelling, Response Surface Methodology (RSM), Stamping Test

1. INTRODUCTION

In the process parts in stamping, especially in multistep stamping, it is difficult to determine the shape structure, material state, and stress and strain. Usually the process parameters are verified by trial production, which is a time consuming and expensive. Computer-aided engineering (CAE) analysis technology of metal plastic forming based on the finite element method (FEM) is important for reducing the dependence of design experience of the stamping process and improving reliability [1-3].

CAE analysis in sheet metal stamping is widely used in single-step stamping analysis [4-7], and CAE analysis of the multistep stamping process and the application of the response surface methodology (RSM) to optimise the parameters of the multistep stamping process are current popular research subjects [8-10]. RSM combines mathematical and statistical methods to describe system response as a surface on a variable area. Unlike general optimisation methods, RSM can study variable interactions while reducing test times. Thus, this method is widely used in product development and design [11, 12].

For successful micro-channel forming in a two-stage forming approach, Bong et al. [13] selected the effects of punch radius, die radius, and forming depth as process variables, and their effects on formability were investigated by finite element simulations, experiments, and RSM. The optimal forming process agreed well with experiments. Azaouzi et al. [14] described a numerical method for designing multistep stamping tools. The proposed method is based on RSM and the sequential quadratic programming algorithm, by which the authors reduced the number of forming steps and increased process productivity. Mostafapour et al. [15] developed a second-order statistical model to show the relationship between drawing depth and input variables by RSM to eliminate wrinkling and fracture in the deep-drawing process. Lang et al. [16] conducted a RSM-based optimisation to obtain the optimized process parameters of hydro-forming for vehicle closure panels. The panels were produced successfully using the optimised

process parameters. In short, RSM is widely used in the optimisation of stamping process parameters to reduce the time and cost, and the conclusions obtained are specific to a certain product.

Due to the asymmetric structure of a spring seat, the stress and deformation during the stamping process is more complicated than that of the symmetrical parts. The technicians can only test the stamping dies and repair them repeatedly in order to obtain reliable process parameters before production. In this study, CAE analysis is used to simulate the complete stamping process to find the defects. Then the cause is analysed, and the process parameters were optimised using RSM.

2. RESEARCH METHODOLOGY

2.1 Characteristic of spring seat and stamping process

As shown in Fig. 1, the spring seat was used to install the damping spring of the automobile suspension system. The three-dimensional structure of the spring seat is shown in Fig. 2. It was a spiral curved structure that was in contact with the spring. The shock absorber was installed in the hole with a straight edge. The appearance requirement of the seat was a smooth transition of the surface without cracks, and the thickness needed to be between 1.4 and 2.2 mm.

Due to the thin-walled structure, spring seat is often produced by stamping process. The raw material of the spring seat is cold-rolled carbon steel SPCC with a thickness of 2 mm. Table I shows the properties of steel.

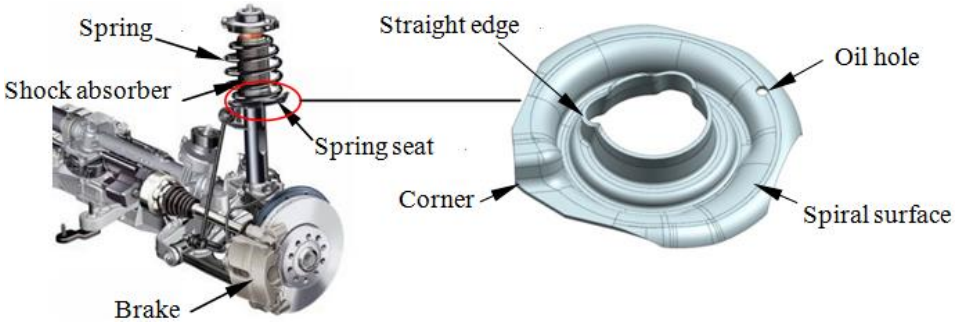

Figure 1: Diagram of suspension system and model of spring seat.

Table I: Properties of SPCC.

Elastic module (GPa)	**Poisson ratio**	**Yield stress** (MPa)	**Strength stress** (MPa)	**Elongation**	**Hardening index**	**Anisotropic**
200	0.3	≤ 210	≥ 270	≥ 38 %	0.18~0.25	1.4~1.6

In the stamping process, holes can be formed by piercing processing and spiral curved can be obtained by forming. To avoid stress concentration, hole flanging was arranged after piercing process. Before piercing, forming is finished. Before forming, drawing, sizing and trimming processes were completed during the multi-position continuous punching .Dies were designed for each stamping process. Fig. 2 shows the expected results after each process was completed.

a) Blank b) Drawing c) Sizing d) Trimming e) Forming f) Piercing g) Hole flanging

Figure 2: Multi-step stamping process of spring seat.

2.2 Simulation results of stamping process

The simulation of stamping process is run on the Dynaform platform. Combined the requirements of seat, dies for each stamping process are designed. Fig. 3 shows the surface of dies for simulation.

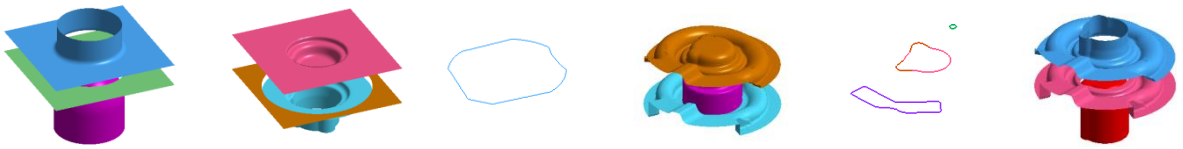

a) Drawing die b) Sizing die c) Trimming die d) Forming die e) Piercing die f) Hole flanging die

Figure 3: Dies for multi-step stamping process.

2.3 Results of original simulation and verification of model

Forming limit diagram and thickening rate for each stamping process were adopted as evaluation indices. Fig. 4 shows the diagram of forming limit.

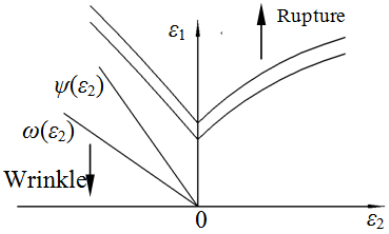

Figure 4: Diagram of forming limit.

Wrinkle evaluation function (D_w) and thickness uneven function (D_t) were decided as the forming quality evaluation functions [17]. D_w can be expressed as follows:

$$D_w = \begin{cases} \sum_{i=1}^{k} \left[\Psi\left(\varepsilon_2^i - \varepsilon_1^i\right)\right]^2, \varepsilon_1^i < \Psi\left(\varepsilon_2^i\right) \\ 0, \varepsilon_1^i \geq \Psi\left(\varepsilon_2^i\right) \end{cases} \quad (1)$$

and D_t can be expressed as follows:

$$D_t = \sum_{i=1}^{k} \left(\frac{t_i}{t_0} - 1\right)^2 \quad (2)$$

where ε_1 is the principal strain, ε_2 is the secondary strain, k is the number of elements, i is the element number, t_0 is the original thickness of steel, and t_i is the thickness of steel after deformation.

For the first simulation, using recommended value for the processing parameters [18], drawing, sizing, trimming and piercing process can obtain qualified results. In forming processes, the spiral surface was wrinkled, as shown in Fig. 5 a. The maximum thickening rate reaches 28.31 % as shown in Fig. 5 b, which exceeds the limit of 20 % of the maximum thickening rate. These two defects were the same as those in a certain factory.

a) Diagram of forming limit b) Diagram of forming thickening rate

Figure 5: Defect analysis of forming process before optimisation.

The processing parameters of the stamping have different effects on product. All of the parameters will cause the model to be highly complex, and the computational demand will be huge. RSM can be used to obtain the functional relationship between the response and multiple variables, and the function estimation value under any combination of conditions can be calculated through the obtained functional relationship. Therefore, RSM has advantages over other optimisation methods.

2.4 Design variables

Considering the real conditions of the process, the die clearance, blank holder force, and friction coefficient were selected as random variables for RSM. According to experience, the value ranges of the die clearance C, blank holding force F, and friction coefficient μ were selected as $1.05\,t \leq C \leq 1.25\,t$ (t is the material thickness), $F = p \cdot A$ (A is the effective pressure-side area, 2 MPa $\leq p \leq$ 2.5 MPa), and $0.1 \leq \mu \leq 0.14$, respectively. In this paper, the die clearance ranged from 2.1 to 2.5 mm, the blank holding force ranged from 9 to 13 kN, and the friction coefficient ranged from 0.08 to 0.16. The factor levels of the design variables were obtained using a central composite design, as shown in Table II.

Table II: Central composite design of factor levels.

Stamping parameters	**Mould clearance *C*** (mm)	**Blank hold force *F*** (kN)	**Friction coefficient μ**
-*r*	2.1	9	0.08
-1	2.18	9.81	0.10
0	2.3	11	0.12
1	2.42	12.19	0.14
r	2.5	13	0.16

3. RESULTS AND DISCUSSION

3.1 Results analysis

The experiment arrangement and results are shown in Table III. The coding values of die clearance, blank hold force, and friction coefficient are x_1, x_2, and x_3, respectively. x_0 represents the constant of the model. The response values of D_w and D_t are denoted as y_1 and y_2, respectively.

Table III: Experiment arrangement and results.

Test number	x_0	x_1	x_2	x_3	y_1	y_2	**Test number**	x_0	x_1	x_2	x_3	y_1	y_2
1	1	1	1	1	11.01	11.65	11	1	0	0	0	12.01	11.54
2	1	1	1	-1	13.53	11.57	12	1	0	0	0	12.13	11.55
3	1	1	-1	1	9.88	11.61	13	1	0	0	0	12.62	11.54
4	1	1	-1	-1	12.42	11.55	14	1	0	0	0	12.7	11.48
5	1	-1	1	1	11.23	11.98	15	1	r	0	0	11.71	11.52
6	1	-1	1	-1	14.47	11.95	16	1	-r	0	0	12.21	12.06
7	1	-1	-1	1	10.5	11.95	17	1	0	r	0	12.98	11.76
8	1	-1	-1	-1	13.2	11.92	18	1	0	-r	0	11.48	11.71
9	1	0	0	0	12.21	11.7	19	1	0	0	r	10.2	11.84
10	1	0	0	0	12.66	11.65	20	1	0	0	-r	14.06	11.76

The variance of y_1 was analysed, as shown in Table IV. $p < 0.0001$ indicates that the model was statistically significant. $p > 0.05$ indicates a lack of fit of the regression between y_1 and x_1, x_2, and x_3. The linear effects of x_1, x_2, and x_3, and the quadratic effects of x_1^2 were significant.

Table IV: Variance analysis of y_1.

Source	Sum of squares	*DF*	Mean square	*F* value	*P* value Prob>*F*
Model	27.27	9	3.03	37.45	<0.0001
x_1	0.85	1	0.85	10.47	0.0089
x_2	3.35	1	3.35	41.4	<0.0001
x_3	22.40	1	22.40	276.96	<0.0001
x_1x_2	7.2e-003	1	7.2e-003	0.089	0.7715
x_2x_3	0.034	1	0.034	0.42	0.5326
x_1x_3	0.097	1	0.097	1.20	0.2996
x_1^2	0.39	1	0.39	4.79	0.0434
x_2^2	0.068	1	0.068	0.84	0.3817
x_3^2	0.16	1	0.16	1.92	0.1956
Residual	0.81	10	0.81		
Lack of fit	0.34	5	0.069	0.73	0.6283
Pure error	0.47	5	0.093		
Cor total	28.07	19			

According to the analysis result, the regression equation for wrinkling evaluation was obtained as follows:

$$y_1 = 12.26 - 0.25x_1 + 0.5x_2 - 1.28x_3 - 0.15x_1^2 \quad (3)$$

With the same method, the regression equation for the uneven thickness function was obtained as follows:

$$y_2 = 11.73 - 0.17x_1 + 0.015x_2 + 0.025x_3 + 0.01x_1x_3 + 0.02x_1^2 \quad (4)$$

3.2 Effects of process parameters on responses

The response surface of the wrinkle evaluation function y_1 with die clearance *C*, blank hold force *F*, and friction coefficient μ is shown in Fig. 6. The wrinkle evaluation function y_1 decreases with increases in die clearance and friction coefficient, but decreasing blank hold force causes y_1 to decrease. y_1 is most affected by the friction coefficient because a high blank hold force leads toa small die gap, which hinders sheet flow. A proper increase in friction coefficient can make sheet metal forming sufficient, thereby reducing wrinkling. The diagram shows that when the blank hold force was between 9.00 and 10.00 kN, the die clearance was between 2.40 and 2.50 mm, the friction coefficient is between 0.14 and 0.16, and a small y_1 can be obtained.

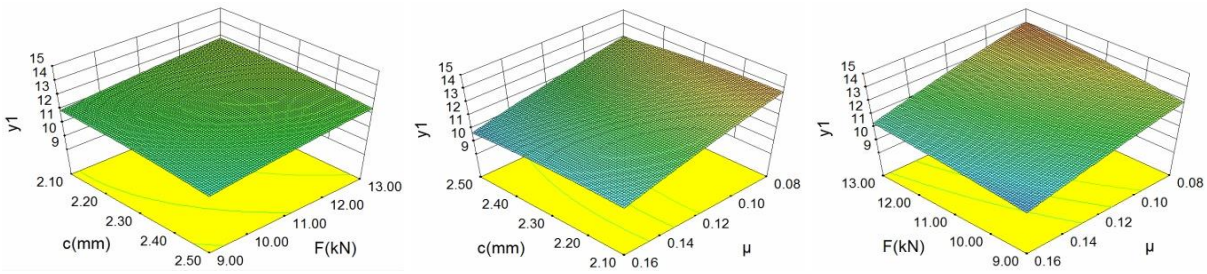

a) *C* and *F* b) *C* and μ c) *F* and μ

Figure 6: Effect of stamping parameters on y_2.

The thickness evaluation function was used to calculate the thickness of each sheet element. The response surface of y_2 with the die clearance C, blank holding force F, and friction coefficient μ is shown in Fig. 7. The thickness unevenness evaluation function y_2 increased with a decrease in the die clearance, decreased with an increase in the blank holding force, and increased with an increase in the friction coefficient. The influence of the die clearance was the most significant. Proper increases in the blank holding force and friction coefficient could improve the resistance uniformity during sheet flow, yielding a uniform sheet thickness. The diagram shows that the die clearance, blank holding force, and friction coefficient should be set to 2.40–2.50 mm, 9.50–12.00 kN, and 0.90–0.14, respectively, to minimise y_2.

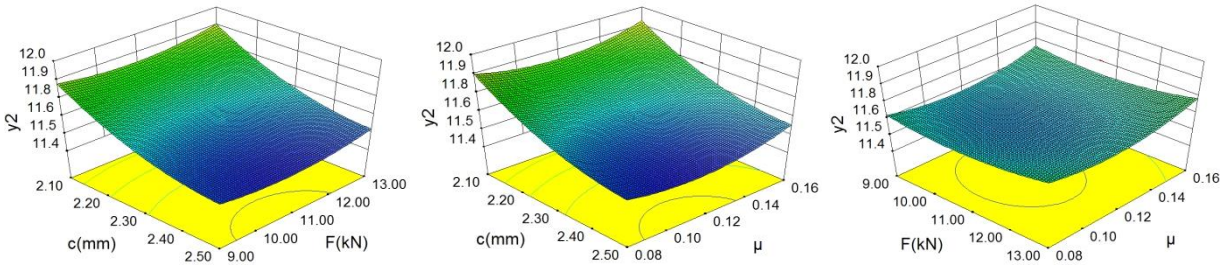

a) C and F b) C and μ c) F and μ

Figure 7: Effect of stamping parameters on y_2.

The target response surface when functions y_1 and y_2 are added by weights of 0.6 and 0.4, respectively, is shown in Fig. 8.The maximum desirability is 0.871, and the obtained parameters were converted into the following stamping parameters: C = 2.42 mm, F = 10.18 kN, and μ = 0.13.

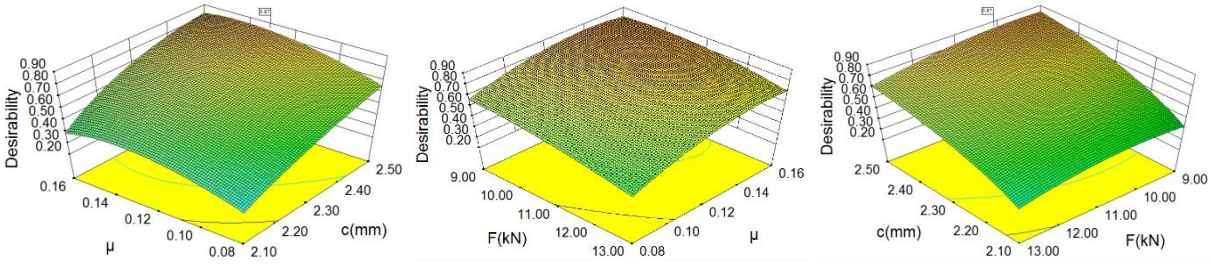

a) C and F b) C and μ c) F and μ

Figure 8: Effect of stamping parameters on desirability.

3.3 Optimised forming results

The numerical simulation of the forming process is performed using the optimized process parameters, as shown in Fig. 9. Unlike the helical surface in Fig. 5 a, the wrinkling region is noticeably reduced, and the area with wrinkling tendency turns into a forming safe zone in Fig. 9 a. A comparison of Figs. 9 b and 5 b indicates that the maximum thickening rate of the helical surface is reduced from 28.31 % to 19.84 %, the area with the higher thickening rate than the other is reduced evidently, and the forming requirement is fulfilled.

a) Diagram of forming limit b) Diagram of forming thinning rate

Figure 9: Forming results after optimisation.

A comparison of the functionsD_w and D_t is shown in Table V. The wrinkling evaluation function D_w decreased significantly by 31.72 %, and the thickness of the uneven evaluation function D_t decreased by 2.85 %. Although the wrinkling areas remained in the spring seat, the sheet thickness was not more than 20 % and did not affect the function of the spring seat. When the spring seat was under working conditions, the abrasion between the helical surface and the spring was intense. Therefore, increasing the thickness by a proper amount was advantageous.

Table V: Comparison of evaluation function.

Comparison	D_w	D_t
Before optimisation	14.47	11.95
After optimisation	9.86	11.59
Decreasing rates	31.72	2.85

3.4 Stamping test

The optimised processes and parameters were used to design the die. Fig. 10 shows the continuous punching process and work piece. Fig. 11 shows the forming process die and product. Fig. 12 shows the pierced and trimmed die and piece. The shape of the helical surface transitioned smoothly. No significant wrinkling on the helical surface or rupture in the flanging structure occurred. The edge of the spring seat did not present any burrs or other defects. Thus, the products satisfied the appearance requirements.

Figure 10: Continuous-punching die and work piece.

Figure 11: Forming die and work piece.

Figure 12: Piercing and trimming die and work piece.

The surface of the sample was tested by placing it on a special tool, as shown in Fig. 13 a. The gap between the sample and tool was used to determine whether the profile met the

requirements. The detection results showed that the surface of the piece fit the surface of the gauge, the edges of the trial parts did not exceed the inspection points, and the location of the oil hole met the requirements.

The flanging structure was detected by a go/no-go gauge, as shown in Figs. 13 b and c. The go gauge, with a 45.3 mm diameter, could pass through the flanging structure, whereas the no-go gauge, with a 45.5 mm diameter, could not pass through. The results of the go/no-go gauge showed that the tolerance of the flanging structure met the requirement.

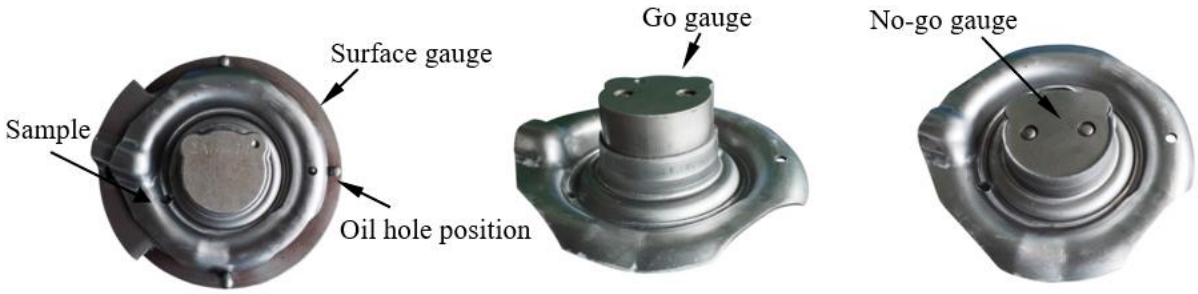

a) Profile verification b) Go gauge test c) No-go gauge test

Figure 13: Gauges for detecting.

4. CONCLUSION

Numerical simulations of the stamping process of spring seat were conducted in this study. Based on the structural characteristics of the seat, processing steps were selected first. With the help of empirical formulas, the parameters for the simulation method were obtained, and simulations were carried out. For defects observed in the simulation, solutions were proposed. Optimised stamping parameters were obtained using RSM to alleviate the wrinkle defects on the helical surface in the forming process. In the forming process, a die clearance of 2.42 mm, a blank holding force of 10.18 kN, and a friction coefficient of 0.13 were selected for the actual stamping, and the prototypes fulfilled the stamping quality requirements.

Although the influences of the process parameters on the stamping quality were considered in this work, the yield stress and hardening index of the material, which can affect the stamping quality and are uncontrollable, were not considered. Moreover numerical simulation of sheet metal stamping is to obtain the blank size parameters and process parameters for die test and cannot be used for mass production. The relationship between the size of the parts and the forming parameters need to be further explored to improve the research of the stamping influence factors.

ACKNOWLEDGEMENT

Supported by Natural Science Foundation of China (Grant No. 51975538).

REFERENCES

[1] Qian, S.; Bai, Z. H.; Hu, W. T.; Lin, W.; Wang, T. L.; Zhang, J. S. (2021). Design and key process simulation of a new type of pipe bending unit, *International Journal of Simulation Modelling*, Vol. 20, No. 3, 559-570, doi:10.2507/IJSIMM20-3-574

[2] Zhang, Q.-C.; Liu, Y.-Q.; Zhang, Z.-B. (2017). A new optimization method for drawbead in sheet forming process based on plastic forming principles, *International Journal of Advanced Manufacturing Technology*, Vol. 92, No. 9-12, 3143-3153, doi:10.1007/s00170-017-0412-0

[3] Yan, H.-J.; Zhang, S.-J.; Liu, Y.-Z. (2015). Parameters optimization for aluminium alloy magnet cover with stamping based on FEM simulation, *Proceedings of the 3rd International Conference*

on Material, Mechanical and Manufacturing Engineering, Guangzhou, 2079-2083, doi:10.2991/ic3me-15.2015.400
[4] Zafar, R.; Lang, L.-H.; Zhang, R.-J. (2015). Analysis of hydro-mechanical deep drawing and the effects of cavity pressure on quality of simultaneously formed three-layer Al alloy parts, *International Journal of Advanced Manufacturing Technology*, Vol. 80, No. 9-12, 2117-2128, doi:10.1007/s00170-015-7142-y
[5] Balla, V. K.; Coox, L.; Deckers, E.; Plyumers, B.; Desmet, W.; Marudachalam, K. (2018). Obtaining manufactured geometries of deep-drawn components through a model updating procedure using geometric shape parameters, *Mechanical Systems and Signal Processing*, Vol. 98, 382-401, doi:10.1016/j.ymssp.2017.05.009
[6] Hu, Q.-H.; Zhang, D.-M.; Fu, H.; Huang, K.-K. (2014). Investigation of stamping process of metallic bipolar plates in PEM fuel cell – numerical simulation and experiments, *International Journal of Hydrogen Energy*, Vol. 39, No. 25, 13770-13776, doi:10.1016/j.ijhydene.2014.01.201
[7] Stadnicki, J.; Wrobel, I. (2015). Numerical effectiveness of the simulation of an automotive body part stamping, *Advances in Mechanical Engineering*, Vol. 7, No. 2, Paper 708434, 8 pages, doi:10.1155/2014/708434
[8] Modanloo, V.; Alimirzaloo, V.; Elyasi, M. (2020). Optimal design of stamping process for fabrication of titanium bipolar plates using the integration of finite element and response surface methods, *Arabian Journal for Science and Engineering*, Vol. 45, No. 2, 1097-1107, doi:10.1007/s13369-019-04232-8
[9] Li, W.-P. (2017). Numerical simulation analysis on drawing forming process of front cross member of automobile top cover, *Journal of Plasticity Engineering*, Vol. 24, No. 2, 118-121, doi:10.3969/j.issn.1007-2012.2017.02.020
[10] Da Silva, A. F.; Marins, F. A. S.; Dias, E. X.; da Silva Oliveira, J. B. (2019). Modeling the uncertainty in response surface methodology through optimization and Monte Carlo simulation: an application in stamping process, *Materials & Design*, Vol. 173, Paper 107776, 13 pages, doi:10.1016/j.matdes.2019.107776
[11] Ghabour, R.; Korzenszky, P. (2022). Linear model of DHW system using response surface method approach, *Technical Gazette*, Vol. 29, No. 1, 66-72, doi:10.17559/TV-20201128095138
[12] Khawaja, A. H.; Jahanzaib, M.; Cheema, T. A. (2020). High-speed machining parametric optimization of 15CDV6 HSLA steel under minimum quantity and flood lubrication, *Advances in Production Engineering & Management*, Vol. 15, No. 4, 403-415, doi:10.14743/apem2020.4.374
[13] Bong, H. J.; Barlat, F.; Lee, J.; Lee, M.-G.; Kim, J. H. (2016). Application of central composite design for optimization of two-stage forming process using ultra-thin ferritic stainless steel, *Metals and Materials International*, Vol. 22, No. 2, 276-287, doi:10.1007/s12540-015-4325-x
[14] Azaouzi, M.; Lebaal, N.; Rauchs, G.; Belouettar, S. (2012). Optimal design of multi-step stamping tools based on response surface method, *Simulation Modelling Practice and Theory*, Vol. 24, 1-14, doi:10.1016/j.simpat.2012.01.006
[15] Mostafapour, A.; Akbari, A.; Nakhaei, M. R. (2017). Application of response surface methodology for optimization of pulsating blank holder parameters in deep drawing process of Al 1050 rectangular parts, *International Journal of Advanced Manufacturing Technology*, Vol. 91, No. 1-4, 731-737, doi:10.1007/s00170-016-9781-z
[16] Lang, L.; Yang, X.; Sun, Z.; Ding, S.; Tong, Z. (2015). Multi-objective optimization of hydroforming process parameters for automotive closure panels based on the response surface method, *Automotive Engineering*, Vol. 37, No. 4, 480-484, doi:10.19562/j.chinasae.qcgc.2015.04.020
[17] Su, C. J. (2011). *Sheet Metal Forming Analysis and Application of CAE-Dynaform Project Application*, National Defense Industry Press, Beijing
[18] Xiao, J. R.; Jiang, K. H. (2011). *Stamping Technology*, China Machine Press, Beijing